International Journal of Nanoelectronics and Materials
Volume 16 (Special Issue) December 2023 [155-168]

Comparison Between Wet and Dry Transfer Fe_2O_3-CNT Hybrid Thin Films as Room-Temperature Liquefied Petroleum Gas (LPG) Sensors

Sutichai Chaisitsak[1,*], Buaworn Chaitongrat[1,2] , Shuhaida Yahud[3,4] and Ahmad Faizal Salleh[3]

[1]Department of Electronics Engineering, School of Engineering,
King Mongkut's Institute of Technology Ladkrabang, Bangkok, Thailand
[2]Department of Robotics and Automation Engineering, Faculty of Technology,
Udon Thani Rajabhat University, Udon Thani Province, Thailand
[3]Faculty of Eletronic Engineering & Technology, Universiti Malaysia Perlis,
Pauh Putra Campus, Arau, Perlis, Malaysia
[4]Centre of Excellence for Advanced Sensor Technology (CEASTech),
Universiti Malaysia Perlis, Arau, Perlis, Malaysia

ABSTRACT

Fe_2O_3-CNT hybrid thin films are promising candidates for room-temperature gas sensors with high sensitivity, rapid response, and recovery times. In this work, we reported the suitable fabrication strategies of Fe_2O_3-CNT hybrid thin films as liquefied petroleum gas (LPG) sensors by comparing the dry (without using aqueous solutions) and wet processes. Fe-CNT hybrid thin films were used as the primary material for synthesizing Fe_2O_3-CNT hybrid thin films, which were then annealed in air at 350oC to create α-Fe_2O_3. Characterizations by X-ray photoelectron spectroscopy, transmission electron microscopy, and field emission scanning electron microscopy (FE-SEM) confirmed the decoration of α-Fe_2O_3 nanoparticles on CNT surfaces. The transfer process had effects on the surface morphology and sensor characteristics. FE-SEM presents that the surface morphology of the wet-transfer Fe_2O_3-CNT films was web-like structures with a highly porous morphology. Whereas the surface morphology of the dry-transferred Fe_2O_3-CNT films was a branch-like structure. The I-V relationship of both annealed wet- and dry- films was non-linear indicating the present of n-type α- Fe_2O_3. Under 5 vol.% of LPG, the wet-transferred Fe_2O_3-CNT films have higher sensitivity (S = ~ 3% $T_{resp.}$= 10 s, $t_{rec.}$= 59s) compared to the dry-transferred Fe_2O_3-CNT films (S = ~ 1.4%, $T_{resp.}$=90s, trec.= incomplete recovery). Moreover, the wet-transferred Fe_2O_3-CNTs could detect LPG concentration at a lower value than 25% of LEL (Lower Explosive Limit) with rapid response and recovery time of 23 s and 49 s, respectively.

Keywords: Dry transfer, FE_2O_3-CNT hybrid thin films, LPG sensors, room-temperature sensors, wet transfer

1. INTRODUCTION

Liquefied petroleum gas (LPG) is a complex mixture of hydrocarbon compounds, which mainly consist of propane (C_3H_8), butane (C_4H_{10}), ethyl mercaptan (C_2H_5SH), and similar sulfuric compounds in small amounts for odorization [1]. LPG is widely used as a combustion material in heaters, cooking equipment, and automotive vehicles. LPG is one of the most harmful gases due to its flammability and explosive nature. The explosion of LPG could have occurred if the gas concentration is within the range between the Lower Explosive Limit (LEL) and Upper Explosive Limit (UEL), with a sufficient amount of oxygen and a source of ignition [2]. The LEL and UEL of LPG are 1.8 and 9.5 vol. % of LPG, respectively [3]. Although there is the addition of an odorant to LPG, however, individuals with hyposmia (partial loss of smell) or anosmia (complete loss of smell) may not be able to smell it due to small amounts. Therefore, LPG sensors are necessary for preventing accidents.

* Corresponding authors: sutichai.ch@kmitl.ac.th

Metal oxide (MOx) is one of the most popular LPG-sensing materials due to its ability to be fabricated in nano sizes. Extensive studies on MOx-based LPG sensor shows that it has high sensitivity, high selectivity, high stability, rapid response, inexpensive, and ease of use. However, most MOx-based LPG sensors require high working temperatures (300-500°C) to ensure high-performance [4-6], thus leading to high-power consumption and changes in the microstructure of MOx nanomaterials. In detection of flammable and explosive gases, the high operating temperature can be dangerous. Therefore, application of MOx as a sensing element in LPG sensors at room temperature is limited. To overcome this limitation, research on the development of room-temperature LPG sensors based on hybrid nanocomposites has gaining attention.

Hybrid nanomaterials based on MOx and carbon nanotubes (CNTs) are one of the most researched combination as each has potential for properties enhancement, such as the electrical conductivity, the porosity, and heterojunction generation in sensing materials [7]. The improvement in sensing performance (high response, high selectivity, and low-operating temperature) of MOx-CNT hybrid compared to other sensor fabricated using a single-material is evident [7-9]. Jia *et al*. reported that an acetone sensor using flower-like Fe_2O_3-CNTs nanocomposites exhibit a greater response and better selectivity than pure Fe_2O_3, at 260°C [9]. MOx-CNT composites-based sensors can be fabricated using both the dry and wet processes. The typical dry process involves synthesizing CNTs and mixing them with MOx nanoparticles by plasma treatment and electron beam evaporation [8]. A typical wet process for fabricating hybrid material-based sensors consists of the MOx-CNT combination by probe sonication and magnetic stringing, film coating process, and heat treatment [5]. MOx-CNTs in liquid form are usually coated onto a substrate using spin-coating, screen-coating, and spray-coating technique. However, an aggregation of metal oxide nanoparticles in hybrid films occurred during the coating process, leading to a decrease in the active sites, subsequently reducing their sensitivity [10]. The search for suitable method for MOx-CNT hybrid material deposition is ongoing to improve gas–sensing performance operating at room temperature. To date, there are no reports available comparing dry- and wet- processes of Fe_2O_3-CNT hybrid materials.

Hematite (α-Fe2O3) is a nanostructure n-type semiconducting metal oxide with a wide bandgap ranging from 1.9 to 2.2 eV [11]. This material has been extensively studied in detection of harmful and toxic gases such as LPG due to its high sensitivity, high selectivity, rapid response, and recovery [5]. Furthermore, CNTs as a sensing element for high-sensitivity gas sensors operated at room temperature because it gives high surface-to-volume ratio, hollow-pipe structure, high electron mobility, high chemical reactivity, and stability [12, 13]. However, pure CNTs-based LPG sensor usually has poor sensitivity, long response time, and incomplete recovery [14].

In this work, we report a study of an ultra-thin Fe_2O_3-CNTs hybrid thin-film LPG sensor. The synthesized Fe-CNT layer was deposited uniformly onto a membrane filter using the mist-chemical vapor deposition (mist-CVD) and were subsequently annealed in the air to create Fe_2O_3 [15, 16]. Nonetheless very few reports on fabrication of Fe_2O_3-CNT thin-film gas sensors are available. To obtain the optimum sensing output, better understanding on the how the fabrication process affects the sensor properties. The surface morphologies of the Fe_2O_3-CNT hybrid thin films produced using both dry and wet process were examined. The fabricated Fe_2O_3-CNT hybrid thin film has demonstrated a potential to be used as LPG sensor element operating at room temperature with rapid response.

2. EXPERIMENTAL METHODS

2.1 Sensing Films Synthesis and Gas Sensor Fabrication

The metallic Fe nanoparticles (NPs) and CNT hybrid thin films were synthesized continuously through mist-CVD deposition. Ferrocene ($Fe(C_5H_5)_2$) and ethanol (C_2H_5OH) were used as the catalytic and the carbon source, respectively [12]. The ratio of ferrocene to ethanol solution was fixed at 0.25 wt.%. When the system was heated to 960°C under atmospheric pressure, the precursor solution was injected into the tube furnace at a rate of 1000 sccm using argon (Ar) as the carrier gas. As-grown Fe-CNTs in the high-temperature zone then moved downstream and were collected onto a mixed cellulose ester (MCE) membrane filter (0.45 μm pore size) at the bottom of the reactor at room temperature (from now on called " as-grown films"). Next, the as-grown films on the membrane filter were transferred using the dry technique by pressing onto a glass substrate without the use of any solvent (water, acetone, or ethanol) (from now on called "dry–transfer films"), as shown in Figure 1a. The wet-transfer method on another hand transferring as-grown films with water, acetone, and ethanol. First, as-grown films were transferred onto a glass substrate by pressing on a substrate as described in the dry-transfer, and then, MCE was removed by dissolving in acetone solutions for 48 hours. Subsequently, the transferred films were washed with ethanol and deionized water several times (from now on called "wet-transfer films"), as shown in Figure 1b. After transferred onto substrates either by dry-transfer or wet-transfer, the transferred films were annealed in the air at 350°C for 8 hours. In this study, the annealing temperature of 350°C to form Fe2O3 was selected, as TGA finding in previous study suggest that at this temperature, the Fe (in CNTs) entirely formed to Fe_2O_3 and contamination (amorphous carbon, carbon case, residual membrane filter) on CNTs were removed [17]. If annealed at a higher temperature, the CNTs are also burned out, leading to the films having extremely high resistance (~ 20 MΩ), which is unsuitable for sensing measurement.

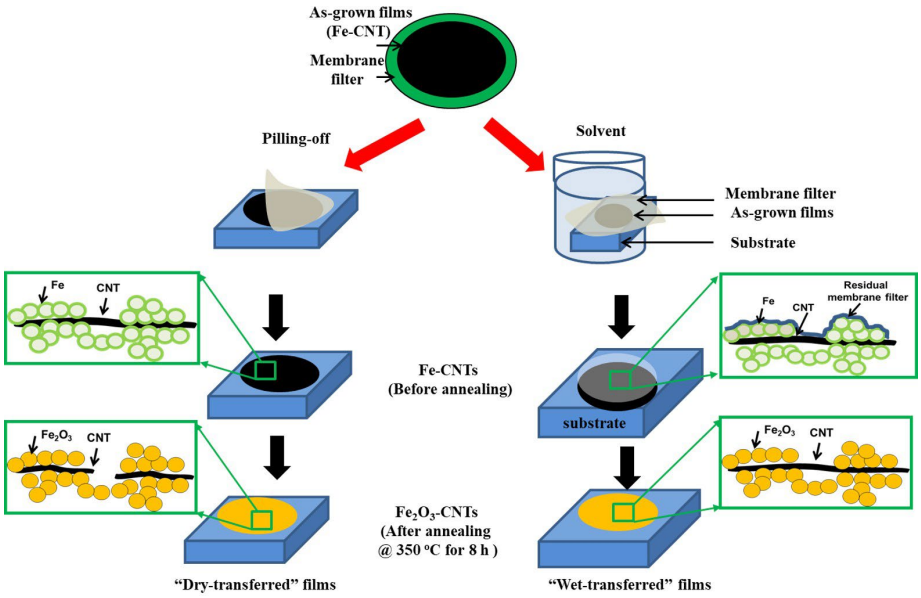

Figure 1. Schematic diagram showing the preparation process of Fe2O3-CNT hybrid thin film. As-grown films were prepared onto the substrate by (a) dry transfer process (the pressing onto a substrate and pilling-off) and (b) wet transfer process (pressing onto a substrate and removing filter with dissolving in acetone solutions for 48 h). Subsequently, both dry-transfer film and wet-transfer films were annealed in air at 350°C to create α-Fe2O3.

2.2 Materials Characterization and Sensor Measurements

The surface morphologies of the hybrid films were investigated using field emission scanning electron microscopy (FE-SEM). The adhered nanoparticles on CNT films were verified via Transmission electron microscopy (TEM). The purity, diameter, and type of CNTs were determined by using Raman spectroscopy. The surface chemical composition and chemical states of Fe_2O_3-CNT films were obtained using X-ray photoelectron spectroscopy (XPS).

After transferring the Fe_2O_3-CNT thin film onto a glass (or Si) substrate, the carbon conductive/Ag electrodes were then aligned on the Fe_2O_3-CNT thin film. The sensing characteristics of the Fe_2O_3-CNTs sensor were investigated at room temperature (approximately 28oC). The fabricated sensors were supplied with voltage ranging from 1 - 5 V throughout the measurements. The changes in resistance of the sensors were measured and recorded via Kelley 2004 source meter. Data acquisitions (DAQ), storage, and plotting in real-time were realized using a personal computer with LabView™ software via a GPIB (General Purpose Interface Bus) interface control. The desired concentration could be achieved by using a mass-flow controller unit. The sensitivity of a gas sensor is defined as the rate of change in the resistance of the sensing film in the presence and absence of gas. The sensitivity (S) for the sensor is given by [18]:

$$S(\%) = \frac{|\Delta R|}{R_g} \times 100 \qquad (1)$$

ΔR is $R_{\$} - R_{\%}$, where $R_{\%}$ and $R_{\$}$ denote the electric resistance value of sensors when exposed to LPG gas and N_2 (or zero air), respectively. The sensors were tested with 5 vol.% of LPG, and further tested for repeated exposure to similar concentration. The sensors performance to different LPG concentration were conducted for 0.1, 0.4, and 0.7 vol.% LPG.

3. RESULTS AND DISCUSSION

3.1 Characterization of Sensing Films

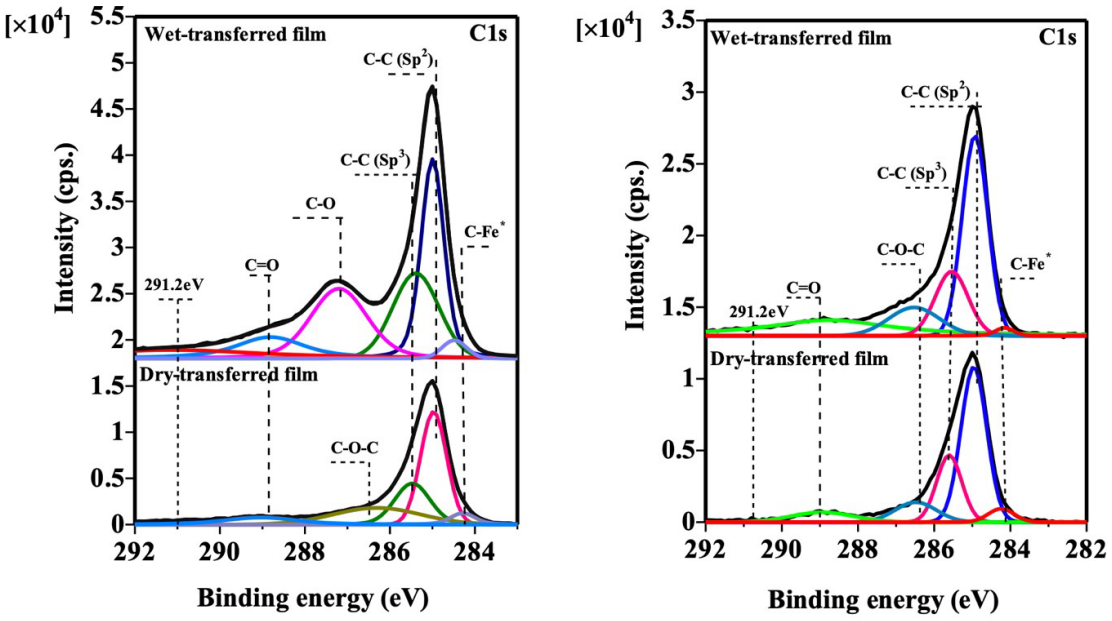

Figure 2. XPS spectra for C 1s states. Wet-transferred and dry-transferred films (a) before annealing (Fe-CNTs) and (b) after annealing (Fe_2O_3-CNT).

The high-resolution C 1s peak of both dry-transfer and wet-transfer films before annealing (Figure 2a) can be deconvoluted into four similar peaks of the binding energy (B.E) located at 284.3, 284.9, 285.4, and 286.3 eV, which correspond to the C-Fe*, sp^2 C-C bonds, sp^3 C–C bonds, and C-O respectively [19, 20]. Except for two peaks assigned to C-O-C (286.3 eV in dry transfer films) and C=O (287.2 eV in the wet transfer film). Moreover, the B.E at 291.2 eV was also observed in both films which is the shake-up satellite peak of the sp2 carbon nanotube [21]. The sp^2 C-C bonds refer to the CNT, whereas the C-O-C, C-O, and C=O bonds indicate the oxygen-containing functional groups and C-Fe* components indicate the carbide. The C=O bonds in the wet-transfer film before annealing (Figure 2a, upper) refer to the remaining organic compounds from the MCE membrane filter. However, the residual MCE membrane filters were removed after annealed at 350°C (Figure 2b, upper). Therefore, after annealing, the high-resolution C 1s peak of the dry- and -wet transferred films (Figure 2b) presents the C-Fe*, sp^2 C-C bonds, sp^3 C–C bonds, C-O-C, and C-O. The sp^2 C-C bonds have a higher intensity than the oxygen-containing functional groups of C-O-C, C-O, or O–C=O because of the abundance CNTs in the film. These high-resolution C 1s peak results indicated that the wet-transferred and dry-transferred films before annealing had similar chemical bonds, except C-O for the wet-transferred film due to the residual MCE membrane filter. However, wet-transferred, and dry-transferred films had similar chemical bonds after annealed in air at 350°C for 8 hrs. The carbon bonds in all films are CNTs.

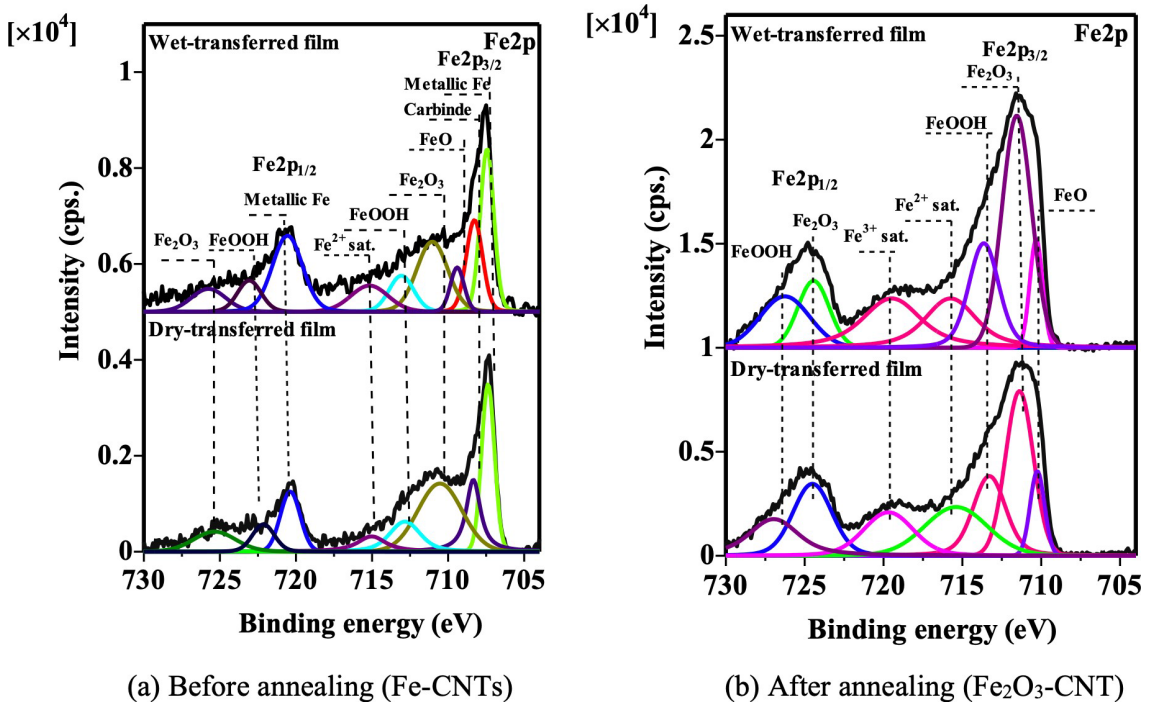

Figure 3. XPS spectra for Fe_2p states. Wet-transferred and dry-transferred films (a) before annealing (Fe-CNTs) and (b) after annealing (Fe_2O_3-CNT).

The high-resolution Fe_2p spectra of the dry-transferred and wet-transferred films before annealing are presented in Figure 3a. Fe^0 peak at 707.4 eV corresponds to the metallic Fe [22], confirming the formation of metallic-Fe nanoparticles in the films before annealing. Moreover, a peak at 708.2 eV can be assigned to carbide species [23]. Fe^{2+} species are presented at B.E of 709.4 eV, which is related to the FeO [24]. Two peaks of the Fe2p spectrum at 711.4 eV and 720.5 eV are attributed to $Fe2p_{3/2}$ and $Fe2p_{1/2}$ spin-orbit peaks of the Fe^{3+} state in α- Fe_2O_3 respectively, which is consistent with experimental data obtained by other authors [25]. The B.E. positions of 713.6 eV and 727.0 eV for Fe^{3+} state in FeOOH [26] [27]. Whereas the peaks at 715.1 eV and 20.5 eV are the shake-up satellites for Fe^{2+} ($2p_{3/2}$) and Fe^{3+} ($2p_{3/2}$), respectively. The metallic-Fe component has a higher intensity than the Fe_2O_3, FeO, and FeOOH. After annealed at 350oC, the $Fe2p_{3/2}$ peak (Figure 3b) can be deconvoluted into main peaks of α- Fe_2O_3, as well as small peaks

of FeO and FeOOH. Moreover, α-Fe_2O_3 showed the highest intensity peak in deconvolution of the $Fe_2p_{3/2}$ peak, confirming the formation of α-Fe_2O_3 in the CNT films after annealed at 350oC.

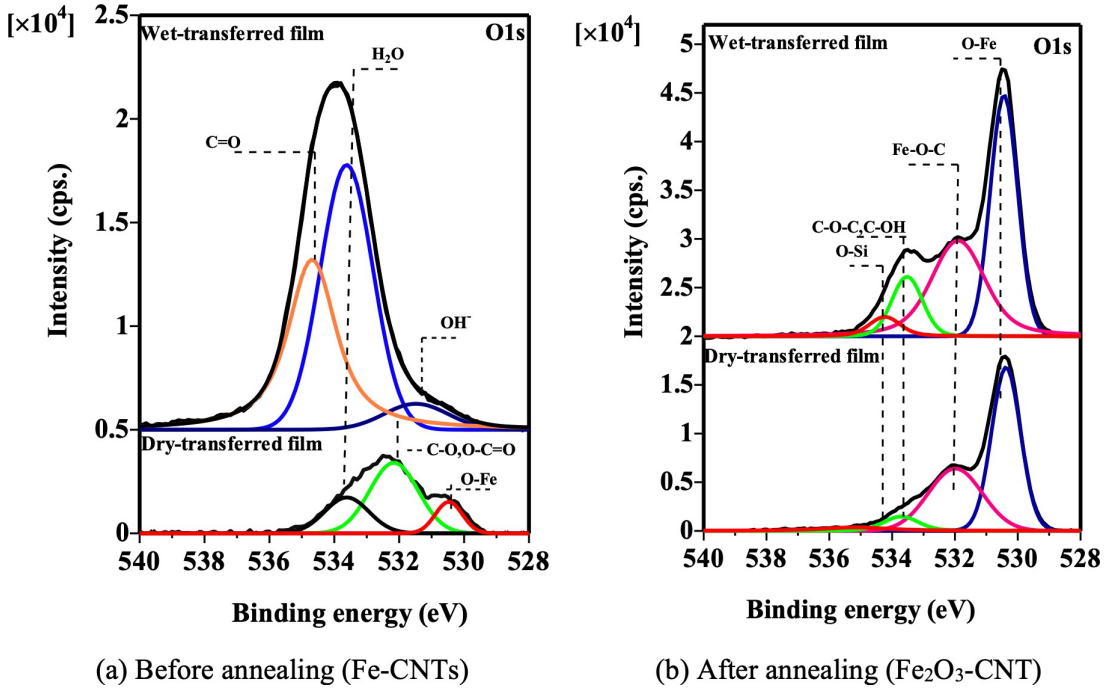

(a) Before annealing (Fe-CNTs) (b) After annealing (Fe_2O_3-CNT)

Figure 4. XPS spectra for O 1s states. Wet-transferred and dry-transferred films (a) before annealing (Fe-CNTs) and (b) after annealing (Fe_2O_3-CNT).

The high-resolution O 1s XPS spectrum of the dry-transferred and wet-transferred films before annealing are shown in Figure 4a. Two similar peaks in both dry-transferred and wet-transferred films before annealing are 530.1 eV and 533.5 eV, assigned to the Fe-O (lattice oxygen species) and C-OH bonds, respectively. Other peaks in the film were assigned to OH- (531.5 eV in the wet-transferred film), C=O (534.5 eV in the wet-transferred film), and C-O (532.3 eV in the dry-transferred film). Note that the C-OH and C=O bonds in wet-transferred films before annealing are due to the MCE-components. However, the wet-transferred and dry-transferred films after annealing had similar O 1s peaks, as shown in Figure 4b. Thus, the result of the C 1s (Figure 2a) and O 1s (Figure 4a) indicated that there are significant differences in the oxygen and carbon states on the surface of dry-transferred and wet-transferred films before annealing; however, after annealed at 350oC both the wet-transferred and dry-transferred films had similar C 1s and O 1s peak shapes.

The FE-SEM and TEM images of as-grown films (Fe-CNT) are shown in Figure 5. It shows that the CNTs were grown like a spider web. The type of CNT is single-wall carbon nanotubes (SWNTs) with a diameter range of 0.9 to 1.9 nm, as estimated from the Raman result [28]. Individual nanoparticles and clusters of small nanoparticles are aligned on the sidewalls of CNTs. These nanoparticles are referring to the metallic Fe as presented in XPS results (Figure 3a). The corresponding TEM image confirms the coexistence of metallic Fe nanoparticles and CNTs, as shown in Figure 5c. It can be seen that the metallic Fe nanoparticles with an average size of 7.33 nm in diameter are widely coated on CNT surfaces.

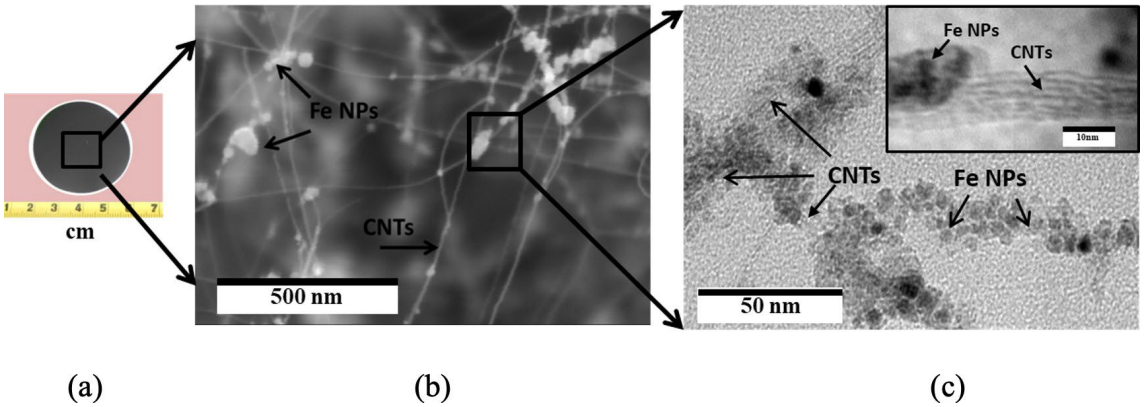

Figure 5. (a) Sample area, (b) FE-SEM image, and (c) TEM image of as-grown films on a membrane filter.

Figure 6 presents the typical surface morphologies of dry-transferred and wet-transferred films before annealing. Figure 6b-1 and 6c-1 show the FE-SEM images at 1μm magnification and figure 6b-2 and 6c-2 show the surface image at 300 nm magnification. Before annealing (Figure 6b), dry-transfer films show a highly porous morphology with a large volume among the CNTs, which is similar to that obtained from as-grown films (Figure 5b). CNTs were formed as web-like structures by accumulating individual CNTs, which are generally attached to small Fe nanoparticles on their surfaces. The similar surface morphology is reasonable due to the SEM imaging of dry-transfer films before annealing were conducted on the top surface (surface previously attached on the MCE membrane filter of as-grown films). Whereas, a typical surface morphologies of the wet-transferred film before annealing (Figure 6c) is a compact mat-like structure due to Van der Waals forces between individual tubes in the solution [29] after immersion in solutions (water, acetone, and ethanol).

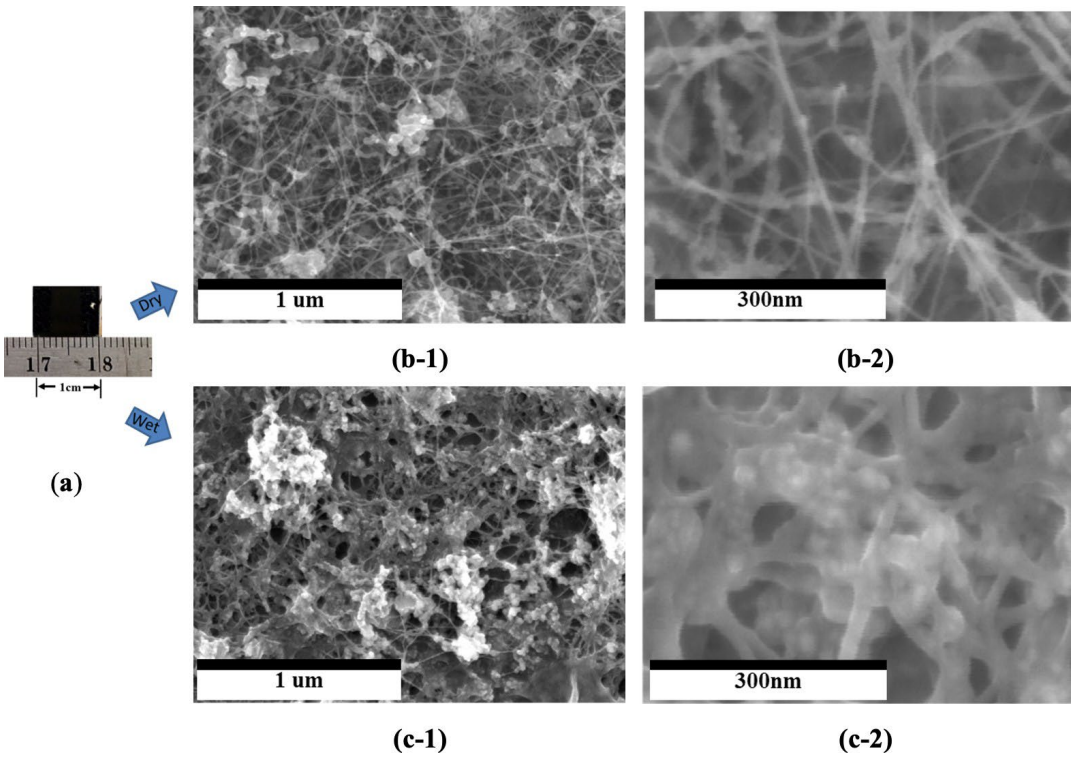

Figure 6. Before annealing, (a) Sample of as-grown films on a substrate after the transfer process. FE-SEM images of (b) the dry-transferred and (c) wet-transferred films.

The impurity (thin jelly-like materials) covered on CNT films was identified as the residual MCE membrane filter, which was detected as C-O in the XPS spectra for C 1s (Figure 2a) and C=O from O 1s states (Figure 4a). The MCE membrane filter in wet-transfer film was not completely removed during immersion in acetone solutions due to the high porosity of CNTs; the MCE membrane filters diffused into the as-grown films and then were linked to Fe and CNTs. However, the residual MCE membrane filter could be eliminated after annealed in air at 350°C (Figure 7c), resulting in the morphology of the films becoming web-like structures. The Raman spectroscopy results calculated the IG/ID ratio of the wet-transfer films before annealing was approximately 4.2; and after annealing was 12.5, indicating the removal of the residual MCE membrane filter and carbon impurities from the Fe_2O_3-CNT thin films after annealing in air at 350oC. Furthermore, dry-transferred film (Figure 7b) presents the discontinuity of CNTs due to the burn-out of CNT during annealing at high temperatures, resulting in a branch-like structure. Figure 7 presents the typical surface morphologies of dry-transferred and wet-transferred films after annealing. Figure 7b-1 and 7c-1 show the FE-SEM images at 1μm magnification and figure 7b-2 and 7c-2 show the surface image at 300 nm magnification.

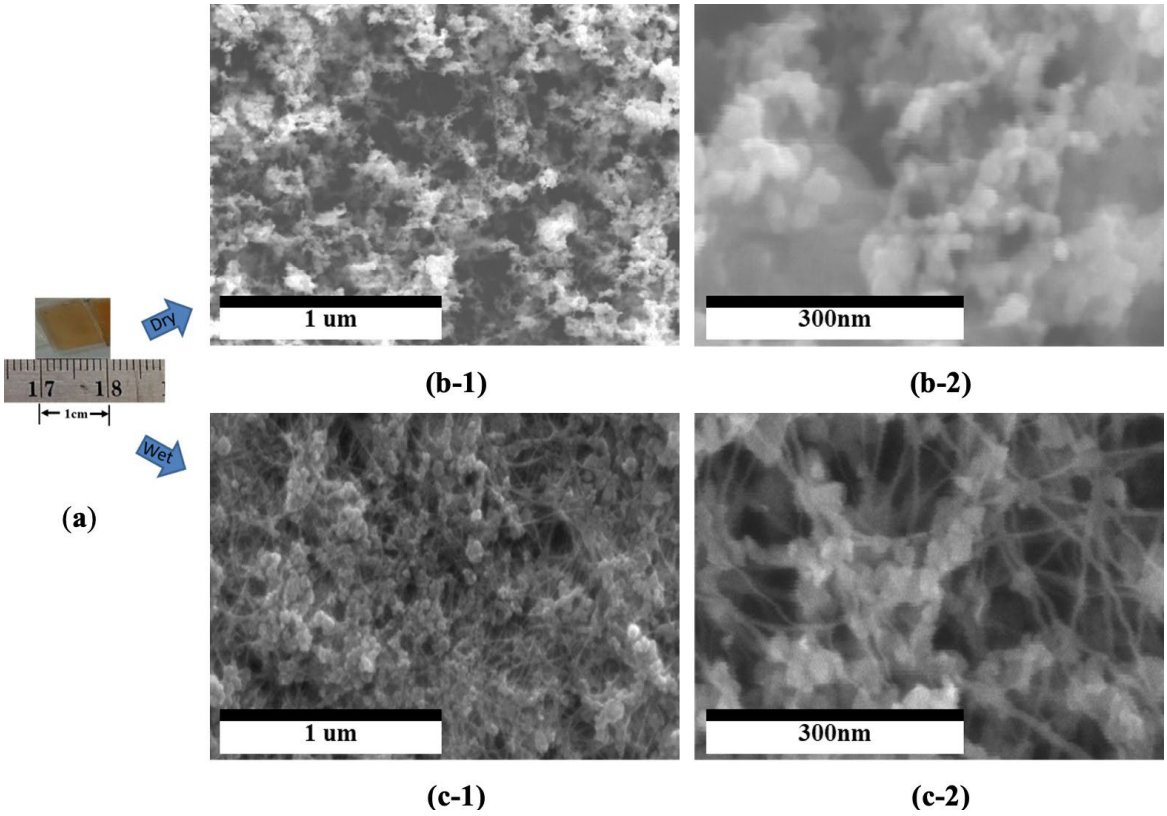

Figure 7. After annealing, (a) Sample of Fe_2O_3-CNT films on a substrate. FE-SEM images of (b) the dry-transferred and (c) wet-transferred Fe_2O_3-CNT films.

The electrical characterization of both FE-CNT and Fe_2O_3-CNT films resistance was carried out using the two points probes [30]. Figure 8a and 8b present the typical current–voltage (I–V) characteristic of dry-transferred and wet- transferred films before and after annealed in air at room temperature, respectively. Both dry-transferred and wet-transferred films before annealing (Figure 8a) shows a linear relation for I-V plot indicating the present of Fe as a good conductor (overshadowing CNTs) as well the good contact between the Fe-CNTs surface and probe electrode. While I-V curves for both dry-transferred and wet-transferred films after annealing showed a nonlinear behavior (Figure 7b) [30]. The observed nonlinear behavior indicates that Fe_2O_3 has formed on CNT surfaces and behaves as a semiconductor for both dry-transferred and wet-transferred films after annealing. In general, resistance values of the dry-transferred films

are greater than that of the wet-transferred films. This is due to the compact mat-like structure observed in the wet-transferred films (Figure 6c), illustrated as the interconnected network established by the individual/buddle CNTs, resulting in numerous electrical paths can be formed [31].

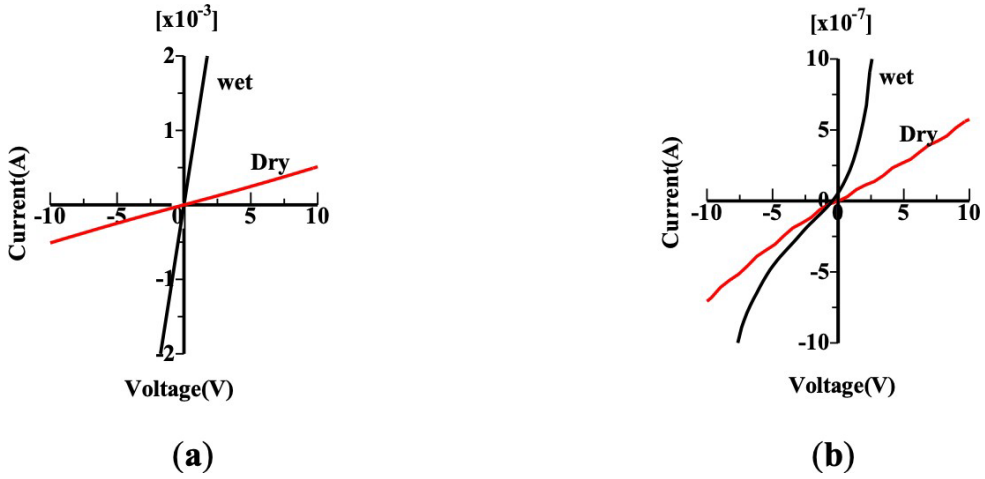

Figure 8. I-V characteristics of (a) the dry- transferred and wet- transferred (Fe-CNT) films before annealing and (b) the dry- transferred and wet- transferred films (Fe_2O_3-CNT) after annealing.

3.2 Sensing Properties

The changes of the dry- transfer and wet- transfer films resistance over time for both before and after annealing towards 5 vol.% of LPG at room temperature are presented in Figure 9. For dry-transferred and wet- transferred films before annealing (Figure 9a), the resistance of both films increased in the presence of LPG, behaving as a p-type material from the CNTs component and small amount of iron oxide shown in XPS spectra in Figure 3. Most of the iron elements before annealed are metallic Fe which is inactive in gas adsorption as the Fe was encapsulated with carbon cages as illustrated in Figure 5b. This result is similar to the resistance change of purified-CNT under reducing gas such as ethanol [32] [33], and ammonia [9]. Under the LPG atmosphere, the resistance of both sensors slowly increased. However, when the supply of LPG was stopped these sensors show incomplete recovery due to the strong binding energy between gas molecules and CNTs sites [34]. Before annealing, the sensitivity of the dry-transferred films was found to be ~ 0.6%, higher than that obtained from wet-transferred films (~0.1%). This result could be due to the residual of MCE membrane filter not completely removed in the wet-transferred films leading to a restriction of gas adsorption on CNTs with poor response.

In contrast to the films before annealing, the response of both annealed dry-transferred and wet-transferred films showed n-type behavior as like the pristine Fe_2O_3 sensor (Figure 9b). These results show that the wet-transferred films after annealed have smoother response curves and show smaller disturbance signals. Furthermore, the annealed wet-transferred films showed a significant rapid response (10s) and recovery time (59s) with a sensitivity of 3%, while the annealed dry-transferred films exhibited a longer response time (approximately 90s) and incomplete recovery time with a poor response (~1.4%). The rapid response and recovery time result could be due to the formation of heterojunction, which can enhance the oxygen absorption [35]; thus, abundant oxygen vacancies are formed on the surfaces of the annealed wet-transferred films, which can provide new active sites for sensing reactions.

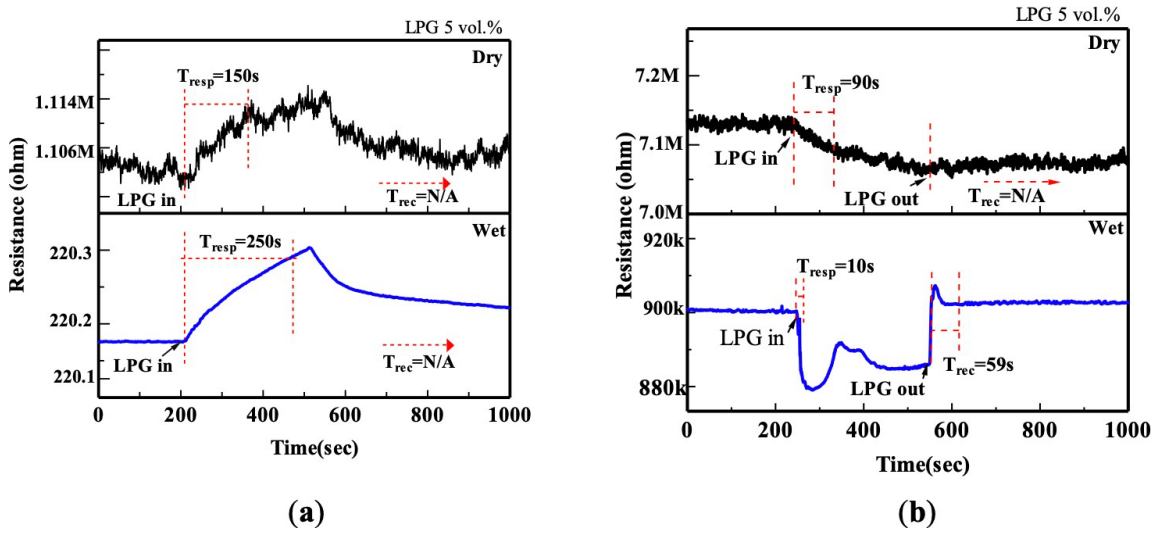

Figure 9. Changes in resistance of (a) Fe-CNT films (before annealing) and (b) Fe_2O_3-CNT film (after annealing) sensors with 5 vol. % of LPG at operating room temperatures.

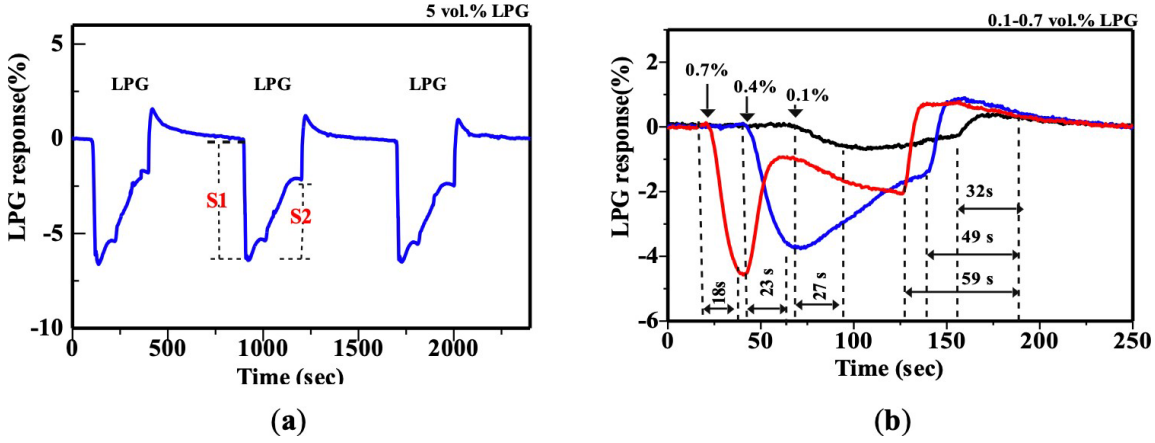

Figure 10. LPG detections at room temperature using the wet-transferred Fe_2O_3-CNT film.
(a) Fe_2O_3-CNT film sensor performance during 3 cycle exposure to 5 vol.% of LPG (diluted with N2).
(b) Fe_2O_3-CNT film sensor performance tested with various concentrations 0.1, 0.4, and 0.7 vol.% of LPG (diluted with zero air).

Figure 10a presents the reproducibility of the annealed wet-transferred films sensor to 5 vol.% of LPG throughout of three cycles of exposure. During exposure to LPG, Fe_2O_3-CNT films both n- and p-type behaviors were observed. “S1” and "S2' are defined as the response of n- Fe_2O_3 and p-CNT type sensors, respectively. These behaviors indicated that the LPG-sensing process occurs in both Fe_2O_3 nanoparticles and CNT materials, in which the LPG-sensing process of Fe_2O_3 is first and then CNTs. Since LPG are adsorbed on the surface of Fe_2O_3 via chemical adsorption while the LPG-sensing process of CNTs is physical adsorption. Moreover, it is observed that sensor response, and response/recovery times were stable and nearly equal at each cycle, indicating good reproducibility of sensing performance.

Figure 10b presents the responses of the annealed wet-transferred films sensors under an air environment with various LPG concentrations diluted in zero air. The sensitivity (with the response and recovery times) of films under LPG concentrations of 0.1, 0.4, and 0.7 vol.% is approximately 4.7% (18s and 59s), 3.7% (23s and 49s), and 0.5% (27s and 32s), respectively. The finding shows that annealed wet-transferred films (Fe_2O_3-CNT films) could detect LPG at concentration levels less than 0.5 vol.% of LPG which corresponds to 25% LEL of LPG.

3.3 Detection Mechanism

The resistance-changing behaviors of as-grown film on substrate after transfer may be attributed to the physical adsorption of LPG molecules on the CNTs. P-type CNT sensing behavior is attributed to charge transfer or electronic interactions between CNTs and adsorbed molecules [36]. For interaction between CNTs and LPG (reducing gas/agent: electron donor), the LPG molecules transfer electrons to the CNTs and further recombine with hole carriers. Therefore, the hole carrier density in the CNTs was reduced and consequently increased the electrical resistance, as presented in Figure 9a.

The resistance-changing behaviors of annealed dry-transfer and wet-transfer films may be attributed to the adsorption and desorption (chemisorption) of LPG molecules on the Fe2O3 and CNT nanocomposite sensing film. The LPG-sensing mechanisms at room temperature could be explained based on the formation of p-n heterojunctions between p-type CNT and n-type metal-oxide-semiconductor of Fe_2O_3. In the air, ambient oxygen adsorbs and captures electrons from the conduction band of Fe_2O_3 and the Fermi level of CNT to generate oxygen adsorbate (O_{2-}) at room temperature shown in Eq. 2 and leading to the formation of surface depletion layers on the interface of the Fe_2O_3-CNT sensing film and cause the high resistance of the sensor in air.

$$O_{2(gas)} \leftrightarrow O_{2(ads)}$$

$$O_{2(gas)} + e^- \leftrightarrow O^-_{2\,(ads)} \quad (2)$$

Upon exposure to LPG, LPG molecules as a reducing gas will react with $O+$ according to the reaction [37] [14]:

$$C_nH_{2n+2} + (3n+1)O^{-1}_{2(ads)} \leftrightarrow nCO_2 + (n+1)H_2O_{gas} + (3n+1)e^- \quad (3)$$

Here, C_nH_{2n+2} represents a mixture of hydrocarbons like propane (C_3H_8; n=3) and butane (C_4H_{10}; n=4). This reaction (Eq. 3) leads to a discharge of electrons into the conduction band of Fe2O3 on the sensor surface. This process results in a decrease in the thickness of the electron depletion layer leading to a decrease in the sensor's resistance. Moreover, electron charges generated on Fe_2O_3 during LPG sensing are transported through the CNT nanostructure since the CNT behaves as the electrical conduction pathway between Fe_2O_3 grain boundaries due to the high carrier mobility of CNT. Furthermore, Fe_2O_3-CNT thin films obtained by wet transfer had a significant rapid response and fast recovery. This result could be attributed to the rapid changes in the p-n heterojunction of n- Fe_2O_3 and p-CNTs hybrid films under the LPG atmosphere.

4. CONCLUSION

Fe_2O_3-CNT hybrid thin films were successfully synthesized and transferred via both dry (without using aqueous solutions) and wet processes and annealed in air at 350°C. FE-SEM and XPS characterizations confirmed the α-Fe_2O_3 on the CNT surface in both films. The FE-SEM results illustrate the surface morphology of the wet-transferred Fe_2O_3-CNT films was web-like structures with a highly porous morphology. This is because the wet transferred Fe-CNT films (primary materials) were covered with the residual MCE membrane filter, which protects CNTs from burning during the air-annealing. The surface morphology of the dry-transferred Fe_2O_3-CNT films was a branch-like structure due to the discontinuity of CNTs. The current-voltage (I–V) characteristic of both the dry- and wet- transferred Fe_2O_3-CNT films showed the nonlinear behavior indicating that Fe_2O_3 formed on CNT surfaces. Under 5 vol.% of LPG atmosphere, Fe_2O_3-CNT films obtained from the wet transfer process showed a significant rapid response (10s) and recovery time (59s) with a sensitivity of 3%, while the Fe_2O_3-CNT films obtained from dry-

transferred exhibited longer response time (>90s), incomplete recovery, and poor response (~1.4%). Furthermore, the wet-transferred Fe_2O_3-CNTs could detect LPG concentration at a lower value than 25% of LEL with a response and recovery time of 23 s and 49 s, respectively.

ACKNOWLEDGEMENTS

This work was supported in part by the King Mongkut's Institute of Technology Ladkrabang (KMITL) Research Fund.

REFERENCES

[1] Lee, I., Bae, D. J., Lee, W. K., Yang, C.-M., Cho, S. W., Nam, J., Lee, D. Y., Jang, A. -R., Shin, H. S., Hwang, J. Y., Hongg, S., Kim, K. S., "Rapid synthesis of graphene by chemical vapor deposition using liquefied petroleum gas as precursor", Carbon, vol 145 (2019) pp. 462-469.

[2] Wang, J., Liang, Y., "Effect of hydrogen the explosion characteristics of liquefied petroleum gas-air mixtures", International Journal of Hydrogen Energy, vol 47, issue 6, (2022) pp. 4255-4263.

[3] Abdullah, A. H., Sudin, S., Ajit, M. I. M., Saad, F. S. A., Kamaruddin, K., Ghazali, F., Ahmad, Z. A., Bakar, M. A. A., "Development of ESP32-based Wi-Fi electronic nose system for monitoring LPG leakage at gas cylinder refurbish plant", 2018 International Cconference on Computational Approach in Smart Systems Design and Applications (ICASSDA), (2018), pp. 1-5.

[4] Anand, K., Kaur, J., Singh, R. C., Thangaraj, R. Thangaraj, "Preparation and characterization of Ag-doped In2O3 nanoparticles gas sensor", Chem. Phys. Lett., vol 682 (2017), pp. 140-146.

[5] Patil, D., Patil, V., Patil, P., "Highly sensitive and selective LPG sensor based on α-Fe2O3 nanorods", Sens. Actuators, B, vol 152, issue 2 (2011), pp. 299-306.

[6] Fazio, E., Spadaro, S., Corsaro, C., Neri, G., Leonardi, S. G., Neri, F., Lavanya, N., Sekar, C., Donato, N., Neri, G., "Metal-Oxide Based Nanomaterials: Synthesis, Characterization and Their Applications in Electrical and Electrochemical Sensors", Sensors, vol 21, issue 7 (2021), art. No 2494.

[7] Baig, N., Kammakakam, I., Falath, W., "Nanomaterials: a review of synthesis methods, properties, recent progress, and challenges", Materials Advances, vol 2, issue 6 (2021), pp. 1821-1871.

[8] Dai, M., Zhao, L., Gao, H., Sun, P., Liu, F., Zhang, S., Shimanoe, K., Yamazoe, N., Lu, G., "Hierarchical assembly of α-Fe2O3 nanorods on multiwall carbon nanotubes as a high-performance sensing material for gas sensors", ACS Applied Materials and Interfaces, vol 9, issue 10 (2017), pp. 8919-8928.

[9] Jia, X., Cheng, C., Yu, S., Yang, J., Li, Y., Song, H., "Preparation and enhanced acetone sensing properties of flower-like α-Fe2O3/multi-walled carbon nanotube nanocomposites", Sensors and Actuators, B: Chemical, vol 300 (2019), art. no. 127012.

[10] Chavali, M. S., Nikolova, M. P., "Metal oxide nanoparticles and their applications in nanotechnology", SN Applied Sciences. vol 1, issue 6 (2019) art. no. 607.

[11] Tofanello A., Shen S., De Souza F. L., Vayssieres L. "Strategies to Improve the Photoelectrochemical Performance of Hematite Nanorod-Based Photoanodes", APL Materials. vol 8, issue 4 (2020) art. no. 040905.

[12] Dresselhaus, M. S., Dresselhaus, G., Saito, R., Jorio, A., "Raman spectroscopy of carbon nanotubes", Physics Report, vol 409, issue 2 (2005), pp. 47-99.

[13] P. J. F. Harris, Carbon nanotube science: synthesis, properties and applications: Cambridge university press, 2009, pp. 146-178.

[14] Norizan, M. N., Moklis, M. H., Ngah Demon, S. Z., Halim, N. A., Samsuri, A., Mohamad, I. S., Knight, V. F., Abdullah, N., "Carbon nanotubes: functionalisation and their application in chemical sensors", RSC Adv., vol 10, issue 71 (2020), pp. 43704-43732.

[15] Hua, C., Shang, Y., Wang, Y., Xu, J., Zhang, Y., Li, X., Cao, A., "A flexible gas sensor based on single-walled carbon nanotube-Fe2O3 composite film", Appl. Surf. Sci., vol 405 (2017), pp. 405-411.

[16] Tavakkoli, M., Kallio, T., Reynaud, O., Nasibulin, A. G., Sainio, J., Jiang, H., Kauppinenb, E. I. Laasonen, K., "Maghemite nanoparticles decorated on carbon nanotubes as efficient electrocatalysts for the oxygen evolution reaction", J. Mater. Chem. A, vol 4 (2016), pp. 5216- 5222.

[17] Chaitongrat, B., Chaisitsak, S., "Novel Preparation and Characterization of Fe2O3/CNT Thin Films for Flammable Gas Sensors", Mater Sci Forum., vol 947 (2019), pp. 47-51.

[18] Goutham, S., Jayarambabu, N., Sandeep, C., Sadasivuni, K.K., Kumar, D.S., Rao, K.V., "Resistive room temperature LPG sensor based on a graphene/CdO nanocomposite", Microchim Acta, vol 186 (2019), art. no. 62.

[19] Okpalugo, T., Papakonstantinou, P., Murphy, H., McLaughlin, J., Brown, N., "High resolution XPS characterization of chemical functionalised MWCNTs and SWCNTs", Carbon, vol 43 (2005), pp. 153-161.

[20] Kim, B. J., Kim, J. P., Park, J. S., "Effects of Al interlayer coating thermal treatment on electron emission characteristics of carbon nanotubes deposited by electrophoretic method", Nanoscale Res. Lett., vol 9 (2014), pp. 1-6.

[21] Matrab, T., Chancolon, J., L'hermite, M. M., Rouzaud, J.-N., Deniau, G., Boudou, J.-P., Chehimi, M. M., Delamar, M., "Atom transfer radical polymerization (ATRP) initiated by aryl diazonium salts: a new route for surface modification of multiwalled carbon nanotubes by tethered polymer chains", Colloids Surfaces A: Physicochemical and Engineering Aspects, vol 287, issue 1-3 (2006), pp. 217-221.

[22] Leedahl, B., Zatsepin, D. A., Boukhvalov, D. W., Green, R. J. McLeod, J. A., Kim, S. S., Kurmaev, E. Z., Zhidkov, I. S., Gavrilov, N. V., Cholakh, S. O., Moewes, A., "Structural defects induced by Fe-ion implantation in TiO2", J. Appl. Phys., vol 115 (2014), 053711.

[23] Bonnet, F., Ropital, F., Lecour, P., Espinat, D., Huiban, Y., Gengembre, L., Berthier, Y., Marcus, P., "Study of the oxide/carbide transition on iron surfaces during catalytic coke formation", Surf. Interface Anal., vol 34 (2002), pp. 418-422.

[24] Fujii, T., De Groot, F., Sawatzky, G., Voogt, F., Hibma, T., Okada, K., "In situ XPS analysis of various iron oxide films grown by NO2-assisted molecular-beam epitaxy", Phys. Rev. B Condens. Matter, vol 59 (1999), pp. 3195-3202.

[25] Mekki, A., Holland, D., McConville, C., Salim, M., "An XPS study of iron sodium silicate glass surfaces", J. Non-Cryst. Solids, vol 208 (1996), pp. 267-276.

[26] Ikram, S., Jacob, J., Mahmood, K., Mehboob, K., Maheen, M., Ali, A., Amin, N., Hussain, S., Ashraf, F., Ilyas, S.Z., "A Kinetic study of Tb3+ and Dy3+ co-substituted CoFe2O4 spinel ferrites using temperature dependent XRD, XPS and SQUID measurements", Ceram. Int., vol 46 (2020), pp. 15943-15948.

[27] Hou, Y., Huang, Y., Hou, S., Ma, S., Liu, Z., Ouyang, Y., "Structural, electronic and magnetic properties of RE3+-doping in CoFe2O4: a first-principles study", J. Magn. Magn. Mater., vol 421 (2017), pp. 300-305.

[28] Chaitongrat, B., Chaisitsak, S., "Fast-LPG Sensors at Room Temperature by α-Fe2O3/CNT Nanocomposite Thin Films", J. Nanomater., vol 2018 (2018) 9236450.

[29] Vuong, N. M., Hieu, N. M., Hieu, H. N., Yi, H., Kim, D., Han, Y.-S., Kim, M., "Ni2O3-decorated SnO2 particulate films for methane gas sensors", Sens. Actuators, B, vol 192 (2014), pp. 327- 333.

[30] Barnett, C. J., Gowenlock, C. E., Welsby, K., White, A. O., Barron, A. R., "Spatial contamination- dependent electrical properties of carbon nanotubes", Nano Lett., vol 18, issue 2 (2018), pp. 695-700.

[31] Maria, K. H., Mieno, T., "Production and properties of carbon nanotube/cellulose composite paper", J. Nanomater., vol 2017 (2017) 6745029.

[32] Penza, M., Rossi, R., Alvisi, M., Cassano, G., Serra, E., "Functional characterization of carbon nanotube networked films functionalized with tuned loading of Au nanoclusters for gas sensing applications", Sens. Actuators, B, vol 140 (2009), pp. 176-184.

[33] Penza, M., Cassano, G., Aversa, P., Antolini, F., Cusano, A., Cutolo, A., Giordano, M., Nicolais, L., "Alcohol detection using carbon nanotubes acoustic and optical sensors", Appl. Phys. Lett., vol 85 (2004), pp. 2379-2381.

[34] Peng, S., Cho, K., Qi, P., Dai, H., "Ab initio study of CNT NO2 gas sensor", Chem. Phys. Lett., vol 387 (2004), pp. 271-276.

[35] Li, Z., Li, H., Wu, Z., Wang, M., Luo, J., Torun, H., Hu, P., Yang, C., Grundmann, M., Liud, X., Fu, Y.Q., "Advances in designs and mechanisms of semiconducting metal oxide nanostructures for high-precision gas sensors operated at room temperature", Mater. Horiz., vol 6 (2019), pp. 470-506.

[36] Donato, N., Latino, M., Neri, G., "Novel carbon nanotubes-based hybrid composites for sensing applications", Carbon nanotubes–From Research to Applications, vol 14 (2011), pp. 229-242.

[37] Reddy, M. S. B., Kailasa, S., Rani, B. G., Jayarambabu, N., Bikshalu, K., Munindra, P., Rao, K.V., "MgO@CeO2 chemiresistive flexible sensor for room temperature LPG detection," J. Mater. Sci.: Mater. Electron., vol 30 (2019), pp. 17295-17302.